Analytical Biochemistry 658 (2022) 114928

Contents lists available at ScienceDirect

Analytical Biochemistry

journal homepage: www.elsevier.com/locate/yabio

Ultrasensitive aptamer-functionalized Cu-MOF fluorescent nanozyme as an optical biosensor for detection of C-reactive protein

Gona K. Ali [a,b], Khalid M. Omer [a,b,*]

[a] Department of Chemistry, College of Science, University of Sulaimani, Qliasan St, 46002, Sulaimani City, Kurdistan Region, Iraq
[b] Center for Biomedical Analysis, Department of Chemistry, College of Science, University of Sulaimani, Qliasan St, 46002, Sulaimani City, Kurdistan Region, Iraq

ARTICLE INFO

Keywords:
C-Reactive proteins
Covid-19 biomarkers
MOF
Aptasensor
RNA

ABSTRACT

In the present work, an aptasensing method based on integration of RNA on Cu-MOF was developed for detection of C-Reactive Protein (CRP). Cu-MOF showed stimulated fluorescence and mimetic peroxidase enzymatic activity at the time and can be used as dual-signal transduction. CRP binding RNA was used as a highly selective recognition element and immobilized on the Cu-MOF. The immobilized RNA can block the peroxidase activity and fluorescence of the signal traducer probe. Adding CRP to the RNA/Cu-MOF will release RNA from the surface of Cu-MOF and recover both the stimulated fluorescence and peroxidase activity. A biosensor was built for detection of CRP using the two modes of transduction, either colorimetry or fluorometry. A dynamic linear range was obtained from 0.1 to 50 ng mL $^{-1}$with a limit of detection (LOD) as small as 40 pg mL $^{-1}$was calculated in fluorescence mode and 240 pg mL $^{-1}$ as LOD in colorimetry mode. The LODs are lower than the LOD of nephelometric techniques used in clinical practice and is comparable to the normal clinical cutoff value in high-sensitivity CRP assays (1 μg/mL). The aptasensor was successfully applied for detection of CRP in Covid-19 patients with spike recoveries between 84 and 102% and RSD from 0.94% to 2.05%.

1. Introduction

C-reactive protein (CRP) is a pentameric protein synthesized by liver, whose level rises in response to inflammation [1]. CRP is an acute-phase reactant protein that is primarily induced by the IL-6 action on the gene responsible for the transcription of CRP during the acute phase of an inflammatory/infectious process [2,3]. in the wounded or afflicted area, it might produce discomfort, redness, and edema. Inflammation can be caused by autoimmune disorders and chronic diseases [4]. The severe acute respiratory syndrome coronavirus 2 (SARS-CoV-2)-caused new coronavirus disease (COVID-19) outbreak is seeing a significant increase in affected individuals worldwide [5,6]. Generally the normal CRP level within 0–5 mg/L range [7,8]. CRP levels in patients with COVID19 were found to be significantly higher, ranging from 20 to 50 mg/L on average [9,10].

In clinical diagnosis, it is always paramount to have a reliable, sensitive, and specific method for detection of CRP. Enzyme-linked immunosorbent assay (ELISA) has always been the ''the best standard way'' for the detection and quantification of CRP. However, various other CRP assay formats have also been developed in the last decade [11,12], such as immunoturbidimetry [13], piezoresistive cantilever-based immunoassay [14], Lateral flow assay [15], chemiluminescent immunoassay [16], Reflect-metric interference spectroscopy [17], homogeneous bead-based immunoassay [18], surface Plasmon resonance [19], impedimetry [20,21], and microfluidics [22]. Regardless of their advantageous, the aforementioned methods have some drawbacks, such as long time detection, expensive and complicated instrument, trained personnel, and very delicate for pH and temperature changes. Thus, one should look for better alternative especially for an early-stage diagnosis that need highly sensitive method.

Recently, aptamer-based methods have received much attention in virtue of its high sensitivity, specificity, stability, versatility, and low-cost. [23–26].

Aptamers are single-stranded oligonucleotides that fold into specific structures and bind to specific targets like proteins [27–29]. Due to high specificity, aptamers have utilized in a wide range of biosensors, such for detection of ions [30], proteins [31], enzymes [32], hormones [33].

Nanozymes, and/or mimetic enzymes, showed as promising artificial biocatalysts in bioassays [34]. They are easy-tailored, stable under hard conditions, low-cost, and highly catalytic active that are promising alternative for natural enzymes [35,36]. Among the nanomaterials that have been used recently as nanozymes is Metal Organic Frameworks

* Corresponding author. Department of Chemistry, College of Science, University of Sulaimani, Qliasan St, 46002, Sulaimani City, Kurdistan Region, Iraq.
E-mail address: khalid.omer@univsul.edu.iq (K.M. Omer).

https://doi.org/10.1016/j.ab.2022.114928
Received 26 July 2022; Received in revised form 15 September 2022; Accepted 20 September 2022
Available online 24 September 2022
0003-2697/

(MOFs). They are porous crystalline structures generated by organic ligands that are coordinated with metal atom nodes on a periodic basis. MOFs have a well-defined structures, unique catalytic and surface properties, tunable design, and presence of active sites that is easily accessible [37–40].

The integration of nucleic acid aptamers, ssDNA and/or RNA, with MOFs results to the production of nanostructured bio-interface synergizing the functionalities of both aptamer and MOFs [41–43]. MOF's homogeneous crystalline structure and large specific surface areas allow a wide range of ssDNA and/or RNA to adhere to the surface. Furthermore, MOFs' variable pore diameters allow different types of nucleic acids with varying specificities to be immobilized on their surface or inside the pores [44–46]. Because of the variety of MOFs and aptamers, a wide range of MOF-based aptasensors have been developed, each with its own set of benefits, such as high sensitivity, selectivity, miniaturization and visual detection potential. Aptasensors based on MOFs have been used in a variety of applications, such as clinical diagnostics [47], disease treatment [48], POC testing [49,50], and environmental contamination surveillance [51]. Recently, MOF-based aptasensors have been used to monitor CRP using electrochemical [52], photo-electrochemical detection [53].

Dual-mode detection is highly important in bioanalysis due to possibility to use both at a time and/or any of them [54,55]. Both colorimetry and fluorimetry have advantages and disadvantages that could complement each other's capabilities in dual-mode detection. Thus, sensors with dual-mode detection property are more robust and rugged than mono mode detection.

Based on the discussion above, one can rationally design an aptamer-MOF combination to collect many properties in one nanocomposite such as high affinity from aptamer, enzymatic properties and fluorescence emission from MOFs. Herein, a hydrothermal method was used to prepare stimulated fluorescent/peroxidase nanozyme of Cu-based MOF (Cu-MOF). CRP specific RNA strains were immobilized on Cu-MOFs to block enzymatic activity and fluorescence of the MOF. Later on, turn on mode assay was used via addition of CRP to recover both the stimulated fluorescence and mimetic enzyme behavior. Scheme 1 shows the diagram of the preparation and detection of our proposed biochemical sensor. To the best of our knowledge, this is the first report about MOF-based aptasensor for CRP detection using optical method.

2. Experimental section

2.1. Instruments

UV–Vis absorption spectra were recorded on a Cary 60 Spectrophotometer (Agilent technologies, USA). Fluorescence measurements (PL) were recorded on Cary Eclipsed Fluorescence Spectrophotometer (Agilent Technologies, USA). Field emission scanning electron microscopy (FE-SEM) was used for taking the image of the MOF particles (Germany ZEISS Gemini SEM) in Chengdu, China.

2.2. Chemicals

Amine terminal RNA aptamer was synthesized and purified by Bioneer Co. Ltd. (Daejeon, south Korea) with sequences (5′-NH2-(CH2)6-GCC UGU AAG GUG GUC GGU GUG GCG AGU GUG UUA GGA GAG AUU GC-4). Dimethylformamide (DMF), 3, 3′ 5, 5′-Tetramethylbenzidine (TMB), and Terephthalic acid (TA), C. Reactive Protein (CRP) were all purchased from Merck-Sigma-Aldrich (Baden-Württemberg, Germany) and used as received. Cu $(NO_3)_2{\cdot}3H_2O$ and Hydrogen peroxide (H_2O_2) 30% were purchased from Biochem chemopharma Co.Ltd. (Biochem, ZA Cosne sur Loire, France). TE buffer (Tris-EDTA, pH 8.0)

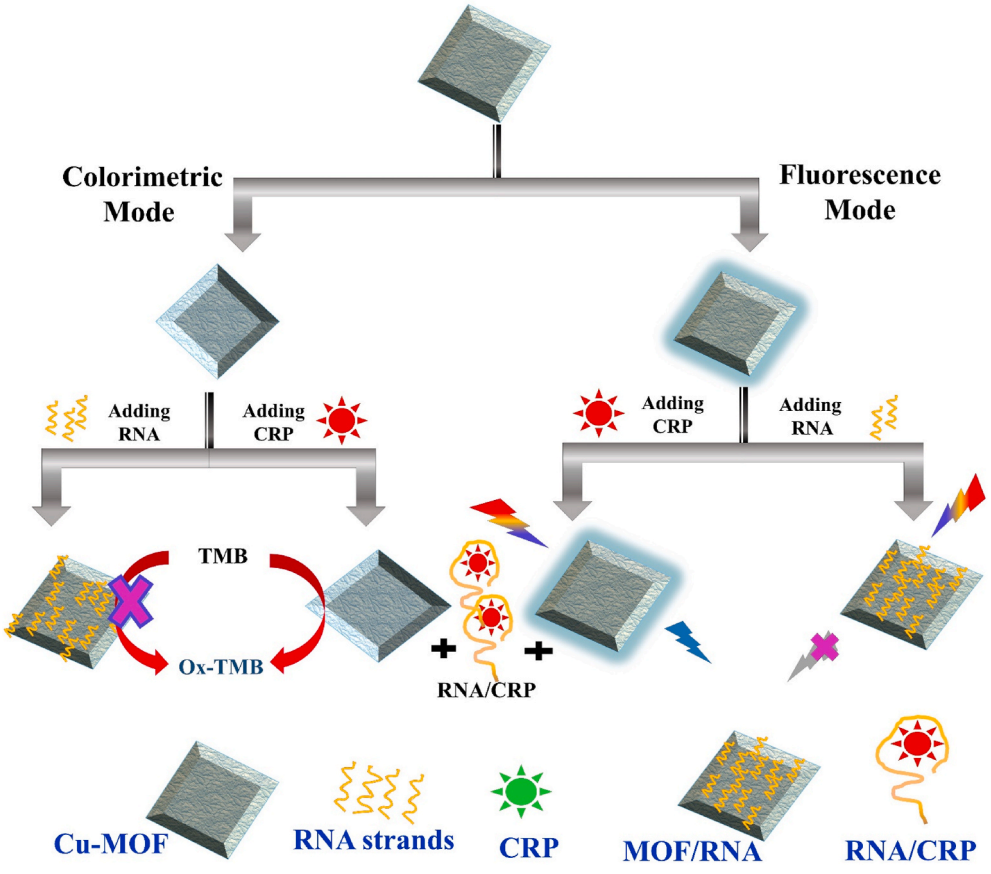

Scheme 1. Schematic diagram of the processes to prepare CRP aptasensor based on RNA on Cu-MOF.

was purchase from EMB Corporation (EMB Co., U.S.A). Phosphate buffer saline (pH 7) was ordered from (CDH Co. Ltd. Delhi, India).

2.3. MOF synthesis

Cu-metal organic framework **(Cu-MOF)** was prepared as in literature with some modifications [56]. In brief, 0.34 g TA and 0.0.49 g Cu $(NO_3)_2{\cdot}3H_2O$ were first dissolved in 10 mL DMF. The resulting solution was then transferred into a 25 mL Teflon-lined stainless-steel autoclave for reaction at 150 °C for 3 h. Blue crystal were collected by centrifugation and rinsed with adequate ethanol and deionized water alternately. To prepare a stock solution of Cu-MOF in water, 10 mg of the Cu-MOF dispersed in 100 mL of deionized water (100 μg mL^{-1}).

2.4. Analysis procedure

For the colorimetric assay, 100 μL of 100 ng mL^{-1} of Cu-MOF solution was mixed with 100 μL RNA (1.0 μM) and then stirred for 2 h at 35 °C. Then to remove the unbounded RNA, the solution was centrifuged. For CRP analysis: different amounts of CRP were added and incubate the solution for 15 min. Later, 100 μL of 5 mM TMB with 100 μL of 30 mM H_2O_2 was added in pH 4 buffer then the absorbance recorded.

For the fluorescence assay, 100 μL of 30 mM H_2O_2 was added to a mixture solutions of 100 μL of 100 ng mL^{-1} of the Cu-MOF and 100 μL RNA (1.0 μM). The solution was stirred for 2 h and centrifuged to remove excesses of unbounded RNA. For CRP analysis: different concentration CRP was added, followed by incubation for 8 h. The fluorescence spectra were measured in room temperature.

3. Results and discussion

3.1. Characterization

FE-SEM was used to image the morphology and size of the Cu-MOF. As shown in Fig. 1, Cu-MOF products have relatively polydisperse decahedral crystal forms in then micrometer to sub-micrometer range (Fig. 1A). EDS elemental mapping and spectra were performed and shown in Fig. 1B–G. It is obvious that the MOF crystals are made of C, O, and Cu, assigning for the formation of Cu-MOF.

3.2. Dual-signal sensing system

Dual-signal sensing based on colorimetric and fluorescence detection for CRP is illustrated Fig. 2. The Cu-MOF has mimetic peroxidase activity and can catalyze colorless TMB to blue colored oxTMB (Fig. 2A, black line). Adding RNA to Cu-MOF solution will block the MOF surface and the mimetic peroxidase activity of the Cu-MOF was diminished (Fig. 2A, red line). Adding CRP protein to the colorless or very faint blue Cu-MOF/RNA solution, results in folding of RNA to CRP and releasing of RNA form the Cu-MOF surface. Hence, peroxidase enzymatic catalytic activity of Cu-MOF will be recovered (Fig. 2A, blue line). Such a turn-on mode can be exploited for establishing a bioassay for CRP.

Interestingly, Cu-MOF shows stimulated fluorescence, not intrinsic, via addition of H_2O_2 and a strong blue emission at 410 can be observed when excited at 320 nm (Fig. 2B, black line). When RNA strand was added, the fluorescence of Cu-MOF was quenched due to immobilization of RNA on Cu-MOF surface (Fig. 2B, red line), and the emission was restored when CRP was added (Fig. 2B, blue line). Such a dual-mode turn on assay, lead us to design colorimetric and fluorometric assay for detection of CRP.

3.3. Optimizations

Various experimental parameters, such as RNA concentrations and stirring time, were examined to achieve the best optimal enzymatic activity. Fig. 3A shows the best RNA concentration study which can affect the enzymatic activity of Cu-MOF. It is shown that 100 nM of the RNA is found as maximum concentration which can stop the whole catalytic activities of the 10 ng mL^{-1} Cu-MOF (Fig. 3A). Moreover, the stirring time effect has been studied in different durations, 0.0, 0.5, 1.0, 2.0, 5.0, 10.0 and 24.0 h. Fig. 3B shows that 2 h of stirring is the optimum time for the RNA to integrate with Cu-MOF and block emission and enzymatic civility. After 5–24 h a slight negligible difference was observed, hence, 2 h was selected as the best stirring time.

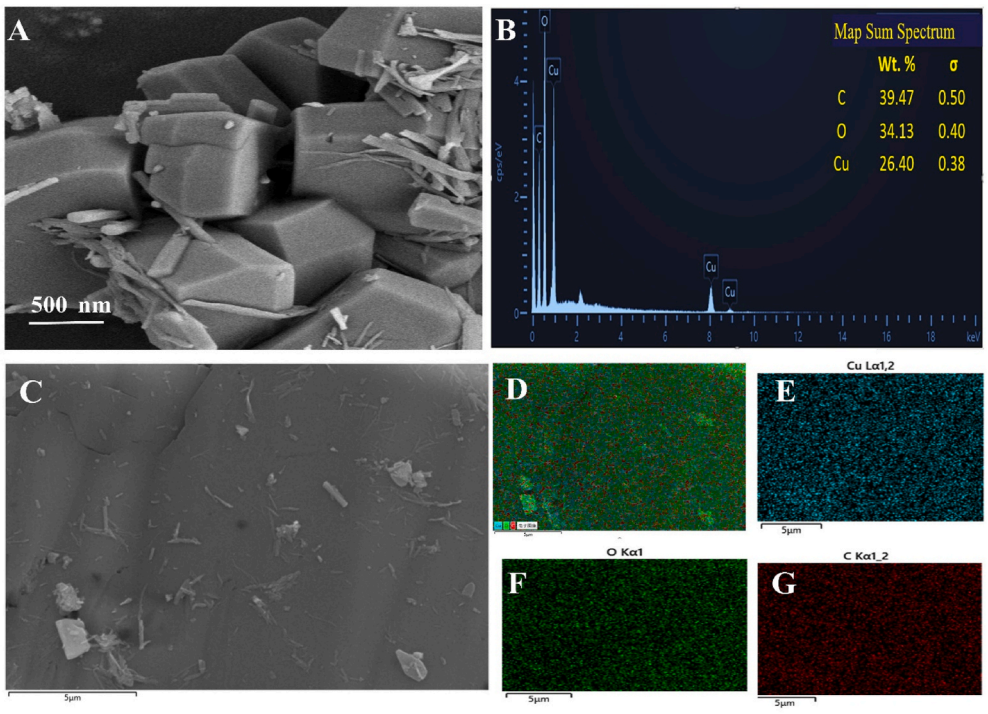

Fig. 1. (**A**) FESEM of Cu-MOF; (**B**), EDX –summation mapping spectra, (**C - G**) and EDX mapping distribution of Cu-MOF at 5 μm scale bar.

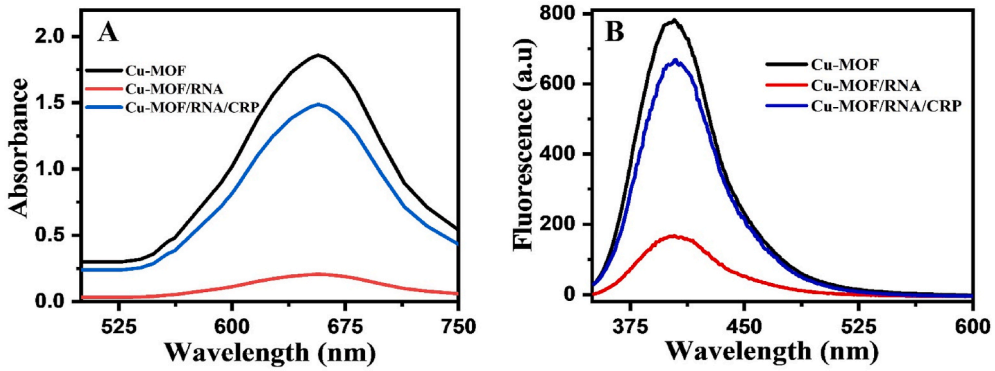

Fig. 2. **(A)** Colorimetric response, **Reaction conditions**: 10 ng mL^{-1} MOF, 0.5 mM TMB, 3 mM H_2O_2, 100 nM RNA. **(B)** Fluorescence response, **Reaction conditions**: 10 ng mL^{-1} MOF, 3 mM H_2O_2, 100 nM RNA.

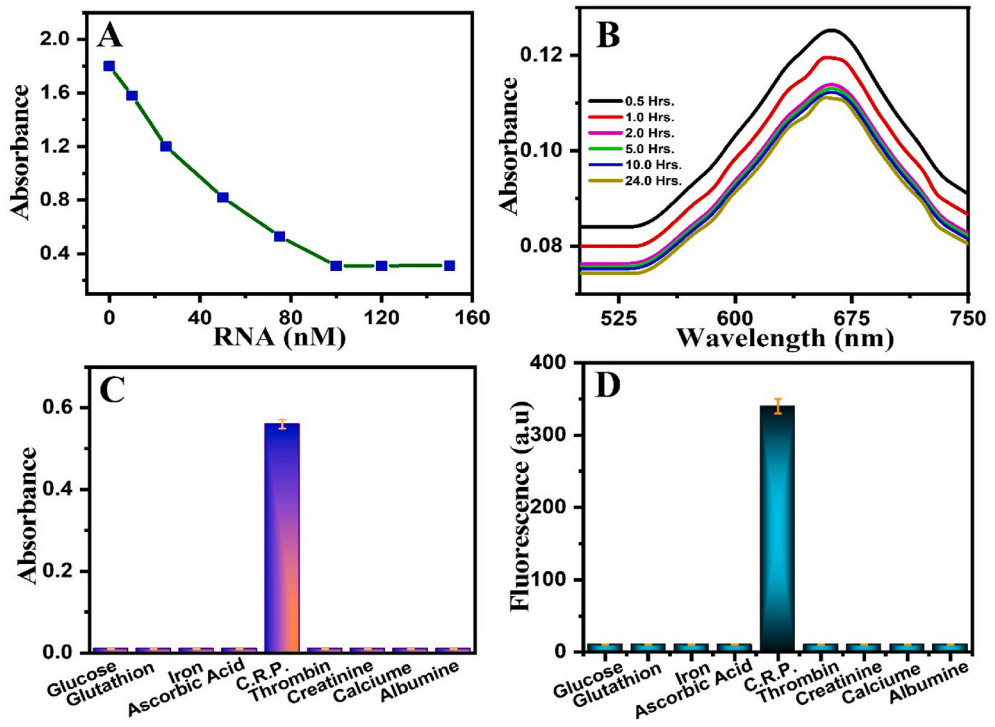

Fig. 3. Optimization studies using 0.1 μg mL^{-1} MOF: **(A)** RNA concentration **(B)** Stirring time study. **(C and D)** Cu-MOF/RNA probe selectivity study toward CRP target where, Cu-MOF (10 ng mL^{-1}), RNA (100 nM), CRP (7.0 ng mL^{-1}), and the concentrations of others interferences are all 700 ng mL^{-1}. **(C)** Colorimetric assay **(D)** Fluorescence assay.

3.4. Selectivity study

The common ions, biomolecules, and proteins present in the serum matrix with CRP were examined. Possible interreference such as glucose, glutathione, ascorbic acid, iron, creatinine, albumin, and calcium, were chosen for this study in order to investigate the tests of selectivity of our biosensor. All of possible interferences were 100 times more concentrated than CRP in the selective trials. Absorbance and fluorescence intensity were substantially higher than the other interferences, as seen in Fig. 3C and D. These findings showed that the Cu-MOF/RNA sensor has a high selectivity for CRP detection in the human serum matrix, making it a promising biosensor for real serum fluid samples.

3.5. Quantitative determination of CRP

For the colorimetric assay, adding different concentrations 0.0, 0.5, 1.0, 2.0, 3.0, 5.0, 10, 20, 50 ng mL^{-1} of the standard CRP to the biochemical reaction system Cu-MOF/RNA. Increasing the intensity of blue color due to oxidation of TMB to oxTMB was observed and the recovery will be almost near to the Cu-MOF signal (Fig. 4A). A linear relationship plot obtained between the absorbance versus the different concentration of CRP with very low limit of detection LOD as 240 pg mL^{-1} and limit of quantification (LOQ) as 750 pg mL^{-1} (Fig. 4B). The LOD, and LOQ has been determined according to S/N = 3 and S/N = 10 criteria respectively (S was estimated to SD (n = 10) obtained from the current intensity of the lowest concentration of CRP in the calibration 0.5 ng mL^{-1}) For the fluorescence assay, same as in the colorimetric assay, different amount of CRP concentrations were added 0.0, 0.5, 1.0, 2.0, 3.0, 5.0, 10, 30, 50 ng mL^{-1} to the integrated Cu-MOF/RNA probe and different fluorescence intensities recovery observed and recorded as shown in Fig. 4C. A linear relationship plot of CRP proteins concentration dependent verses fluorescence has been estimated with LOD 40 pg mL^{-1} and LOQ 130 pg mL^{-1} were measured (Fig. 4D).

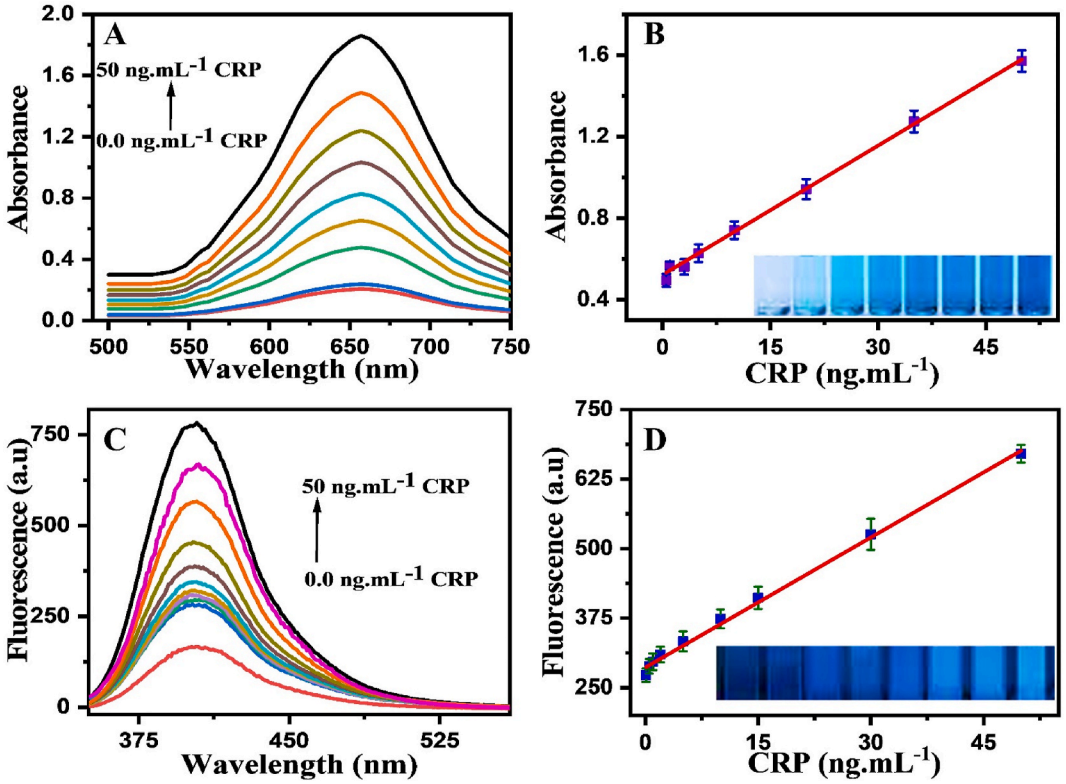

Fig. 4. (**A**) UV–Vis absorption spectra obtained from MOF/RNA-based colorimetric oxidation of TMB in the presence of CRP at various concentrations. (**B**) Plot of the absorbance at 652 nm versus the concentration of CRP, error bars represent the standard deviation of three independent measurements. (**C**) Fluorescence spectra of MOF/RNA probe incubation with different concentrations of CRP (**D**) plot of Fluorescence with excitation 320 nm and emission at 350 nm, versus different concentrations of CRP.

Thus, dual-mode, colorimetry and fluorimetry, offer different linearity and LODs, which is highly useful for multi-use analysis. In other words, for more sensitive level of CRP, one can use fluorescence-based while for higher level, colorimetry is a good option.

4. Applications

Our proposed biosensor was applied for patients with COVID-19 disease. Shahid-Hemn Hospital (Slemani City, Kurdistan Region, Iraq) provided the serum samples. The proposal of the research was approved by the Ethics Committee of the hospital. The samples were collected from the emergency and the intensive care units of the hospital. Patient serums were spiked with standard CRP concentration. The serum samples have been diluted 10 times (0.1 mL of the serum were completed to 1 mL by double deionized water), and were measured for three replicates (n = 3). Table 1 shows that the spike recoveries of CRP ranged for colorimetric-based assay from 84% to 102%, and for the Fluorescence-based assay are ranged between 88% and 94.2%. Spike recovery showed that our proposed method is accurate and can be applied to the real samples of COVID-19 patients. Table 2 shows some published reports for detection of CRP using various methods and techniques. It is obvious that our method is comparable and relatively close to them. The intra-assay precision reached the RSD of 2% (n = 3) for the same day and the inter-assay precession reached 5% (n = 3) for our aptasensor conducted different days.

Table 1
Illustrate the various colorimetric and fluorescence recovery intensities obtained for CRP.

Sample	Unspiked (ng. mL^{-1})	Added (ng. mL^{-1})	Found (ng. mL^{-1})	Recovery %	RSD %
Colorimetric assay					
1	5.61 ± 0.02	5	9.80 ± 0.01	84.0 ± 1.52	1.01
	19.80 ± 0.03	10	30.01 ± 0.04	102.0 ± 1.03	2.01
2	6.42 ± 0.04	5	11.32 ± 0.10	98.0 ± 2.07	1.65
	21.4 ± 0.13	10	31.45 ± 0.05	100.5 ± 1.95	0.94
Fluorometric assay					
1	4.20 ± 0.02	5	8.49 ± 0.05	93.00 ± 2.16	1.82
	8.60 ± 0.02	10	21.00 ± 0.11	88.00 ± 1.38	2.05
2	5.56 ± 0.02	5	10.98 ± 0.14	94.2 ± 2.46	1.63
	20.98 ± 0.01	10	30.01 ± 0.01	90.24 ± 2.63	2.03

5. Conclusions

A novel aptamer-functionalized Cu-MOF-based optical biosensor for CRP detection was developed. CRP binding RNA was immobilized on stimulated fluorescent and peroxidase Cu-MOF. Dual-mode optical detection, colorimetry and fluorometry, was successfully fabricated and used for detection of CRP with high selectivity in serum of COVID-19 patients. The biosensor provided 40 pg mL^{-1} as LOD in fluorescence-based mode and 240 pg mL^{-1} LOD in colorimetric mode. Our probe is highly stable, selective, sensitive, and low-cost precursors which make the probe highly useful for mass-production CRP detection assay. Due to many figures of merits in our proposed method we can apply it in clinical settings, either in a solution or can be deposited on paper in future work.

Table 2
Comparison for CRP detection using various methods with our Cu-MOF-RNA aptasensor.

Biosensor probes	Type of aptamer	Methods of detection	LOD	Ref.
NH_2–Ni-MOF	ssDNA	Electrochemical	0.029 pg mL^{-1}	[52]
ZnO/MPC-Immunosensor	RNA	Electrochemical	5.0 pg mL^{-1}	[34]
$Mn_3(PO_4)_2$/aptamer nanosheet	ssDNA	Electrochemical	0.37 pg mL^{-1}	[57]
2D porphyrinic covalent organic frameworks	ssDNA	Photoelectrochemical	0.1 ng mL^{-1}	[53]
Aptamer-antibody sandwich assay	ssDNA	Fluorescence	2.78 nM	[58]
Aptamer/AuNPs	ssDNA	Fluorescence	380 pM	[59]
Sandwich aptamer	ssDNA	Electrochemical	26 pM	[60]
Sandwich aptamer/ immunoassay	ssDNA	Electrochemical	5.4 * 10^{-2} mg L^{-1}	[61]
Cu-MOF	RNA	Fluorescence	40 pg mL^{-1}	This work
Cu-MOF	RNA	Colorimetric	240 pg mL^{-1}	This work

Author contribution

Gona K. Ali: design of the work, data collection, analysis and interpretation, and drafting the article. **Khalid M. Omer**: design of the work critical revision of the article and Final approval of the version to be published.

Data availability

Data will be made available on request.

References

[1] Shows, V. S. et al. How to Lower Your C Reactive Protein (CRP) Levels.
[2] V. Valkanova, K.P. Ebmeier, C.L.C.R.P. Allan, IL-6 and depression: a systematic review and meta-analysis of longitudinal studies, J. Affect. Disord. 150 (2013) 736–744.
[3] A. Agrawal, CRP after 2004, Mol. Immunol. 42 (2005) 927–930.
[4] T. Bansal, A. Pandey, D. Deepa, A.K. Asthana, C-reactive protein (CRP) and its association with periodontal disease: a brief review, J. Clin. Diagn. Res.: J. Clin. Diagn. Res. 8 (2014) ZE21.
[5] L. Yang, et al., COVID-19: immunopathogenesis and Immunotherapeutics, Signal Transduct. Targeted Ther. 5 (2020) 1–8.
[6] T.T. Le, et al., The COVID-19 vaccine development landscape, Nat. Rev. Drug Discov. 19 (2020) 305–306.
[7] K. Yoon, S. Ryu, J. Lee, J.-D. Park, Higher and increased concentration of hs-CRP within normal range can predict the incidence of metabolic syndrome in healthy men, Diabetes Metabol. Syndr.: Clin. Res. Rev. 12 (2018) 977–983.
[8] O. Meyer, Anti-CRP antibodies in systemic lupus erythematosus, Joint Bone Spine 77 (2010) 384–389.
[9] P. Mo, et al., Clinical Characteristics of Refractory COVID-19 Pneumonia in Wuhan, China, Clinical infectious diseases, 2020.
[10] Y. Gao, et al., Diagnostic utility of clinical laboratory data determinations for patients with the severe COVID-19, J. Med. Virol. 92 (2020) 791–796.
[11] I. Kushner, J.A. Somerville, Estimation of the molecular size of C-reactive protein and Cx-reactive protein in serum, Biochim. Biophys. Acta Protein Struct. 207 (1970) 105–114.
[12] M. Algarra, D. Gomes, J.C.G.E. da Silva, Current analytical strategies for C-reactive protein quantification in blood, Clin. Chim. Acta 415 (2013) 1–9.
[13] O. Deegan, K. Walshe, K. Kavanagh, S. Doyle, Quantitative detection of C-reactive protein using phosphocholine-labelled enzyme or microspheres, Anal. Biochem. 312 (2003) 175–181.
[14] J.H. Lee, et al., Label free novel electrical detection using micromachined PZT monolithic thin film cantilever for the detection of C-reactive protein, Biosens. Bioelectron. 20 (2004) 269–275.
[15] W. Leung, et al., InfectCheck CRP barcode-style lateral flow assay for semi-quantitative detection of C-reactive protein in distinguishing between bacterial and viral infections, J. Immunol. Methods 336 (2008) 30–36.
[16] M.S. Islam, S.H. Kang, Chemiluminescence detection of label-free C-reactive protein based on catalytic activity of gold nanoparticles, Talanta 84 (2011) 752–758.
[17] H.W. Choi, Y. Sakata, Y. Kurihara, T. Ooya, T. Takeuchi, Label-free detection of C-reactive protein using reflectometric interference spectroscopy-based sensing system, Anal. Chim. Acta 728 (2012) 64–68.
[18] C. Punyadeera, G. Dimeski, K. Kostner, P. Beyerlein, J. Cooper-White, One-step homogeneous C-reactive protein assay for saliva, J. Immunol. Methods 373 (2011) 19–25.
[19] H.-C. Kim, et al., Detection of C-reactive protein on a functional poly (thiophene) self-assembled monolayer using surface plasmon resonance, Ultramicroscopy 108 (2008) 1379–1383.
[20] V. Vermeeren, et al., Impedimetric, diamond-based immmunosensor for the detection of C-reactive protein, Sensor. Actuator. B Chem. 157 (2011) 130–138.
[21] T. Bryan, X. Luo, P.R. Bueno, J.J. Davis, An optimised electrochemical biosensor for the label-free detection of C-reactive protein in blood, Biosens. Bioelectron. 39 (2013) 94–98.
[22] W.-B. Lee, Y.-H. Chen, H.-I. Lin, S.-C. Shiesh, G.-B. Lee, An integrated microfluidic system for fast, automatic detection of C-reactive protein, Sensor. Actuator. B Chem. 157 (2011) 710–721.
[23] T. Mairal, et al., Aptamers: molecular tools for analytical applications, Anal. Bioanal. Chem. 390 (2008) 989–1007.
[24] A.V. Lakhin, V.Z. Tarantul, L. Gening, Aptamers: problems, solutions and prospects, Acta Naturae (англоязычная версия) 5 (2013) 34–43.
[25] G.K. Ali, K.M. Omer, Molecular imprinted polymer combined with aptamer (MIP-aptamer) as a hybrid dual recognition element for bio(chemical) sensing applications. Review, Talanta 236 (2022), 122878.
[26] M. Plach, T. Schubert, Biophysical characterization of aptamer-target interactions, Aptamers Biotechnol. (2019) 1–15.
[27] S. Tombelli, M. Minunni, M. Mascini, Analytical applications of aptamers, Biosens. Bioelectron. 20 (2005) 2424–2434.
[28] K.-M. Song, S. Lee, C. Ban, Aptamers and their biological applications, Sensors 12 (2012) 612–631.
[29] E.J. Cho, J.-W. Lee, A.D. Ellington, Applications of aptamers as sensors, Annu. Rev. Anal. Chem. 2 (2009) 241–264.
[30] W. Guo, et al., Advances in aptamer screening and aptasensors' detection of heavy metal ions, J. Nanobiotechnol. 19 (2021) 1–19.
[31] F.V. Oberhaus, D. Frense, D. Beckmann, Immobilization techniques for aptamers on gold electrodes for the electrochemical detection of proteins: a review, Biosensors 10 (2020) 45.
[32] F. Li, et al., Aptamers facilitating amplified detection of biomolecules, Anal. Chem. 87 (2015) 274–292.
[33] J.G. Bruno, M.P. Carrillo, T. Phillips, A. Edge, Discrimination of recombinant from natural human growth hormone using DNA aptamers, J. Biomol. Tech.: J. Biochem. (Tokyo) 22 (2011) 27.
[34] S. Dong, D. Zhang, H. Cui, T. Huang, ZnO/porous carbon composite from a mixed-ligand MOF for ultrasensitive electrochemical immunosensing of C-reactive protein, Sensor. Actuator. B Chem. 284 (2019) 354–361.
[35] Y. Huang, J. Ren, X. Qu, Nanozymes: classification, catalytic mechanisms, activity regulation, and applications, Chem. Rev. 119 (2019) 4357–4412.
[36] R.D. Isho, N.M. Sher Mohammad, K.M. Omer, Enhancing enzymatic activity of Mn@Co3O4 nanosheets as mimetic nanozyme for colorimetric assay of ascorbic acid, Anal. Biochem. 654 (2022), 114818.
[37] Q. Wang, D. Astruc, State of the art and prospects in metal–organic framework (MOF)-based and MOF-derived nanocatalysis, Chem. Rev. 120 (2019) 1438–1511.
[38] H.-C. Zhou, J.R. Long, O.M. Yaghi, Introduction to metal–organic frameworks, Chem. Rev. 112 (2012) 673–674.
[39] H. Li, M. Eddaoudi, M. O'Keeffe, O.M. Yaghi, Design and synthesis of an exceptionally stable and highly porous metal-organic framework, Nature 402 (1999) 276–279.
[40] Sh Mohammed, S. Ameen, N.M. Sher Mohammed, K.M. Omer, Visual monitoring of silver ions and cysteine using bi-ligand Eu-based metal organic framework as a reference signal: color tonality, Microchem. J. 181 (2022), 107721.
[41] L. Tang, Y. Wang, J. Li, The graphene/nucleic acid nanobiointerface, Chem. Soc. Rev. 44 (2015) 6954–6980.
[42] O.B.A. Shatery, K.M. Omer, Selectivity enhancement for uric acid detection via in situ preparation of blue emissive carbon dots entrapped in chromium metal–organic frameworks, ACS Omega (2022), https://doi.org/10.1021/acsomega.2c00790.
[43] K.F. Kayani, K.M. Omer, A red luminescent europium metal organic framework (Eu-MOF) integrated with a paper strip using smartphone visual detection for determination of folic acid in pharmaceutical formulations, New J. Chem. (2022), https://doi.org/10.1039/D2NJ00601D.
[44] G.K. Mishra, A. Barfidokht, F. Tehrani, R.K. Mishra, Food safety analysis using electrochemical biosensors, Foods 7 (2018) 141.
[45] S. Xie, J. Ye, Y. Yuan, Y. Chai, R. Yuan, A multifunctional hemin@ metal–organic framework and its application to construct an electrochemical aptasensor for thrombin detection, Nanoscale 7 (2015) 18232–18238.
[46] D.D. Liana, B. Raguse, J.J. Gooding, E. Chow, Recent advances in paper-based sensors, Sensors 12 (2012) 11505–11526.
[47] M. Lv, et al., Aptamer-functionalized metal-organic frameworks (MOFs) for biosensing, Biosens. Bioelectron. 176 (2021), 112947.
[48] Z. Xu, et al., Aptamer-functionalized metal-organic framework-coated nanofibers with multi-affinity sites for highly sensitive, selective recognition of ultra-trace microcystin-LR, Talanta 236 (2022), 122880.
[49] Y. Wang, et al., Discovering the enzyme mimetic activity of metal-organic framework (MOF) for label-free and colorimetric sensing of biomolecules, Biosens. Bioelectron. 86 (2016) 432–438.

[50] Z. Karimzadeh, M. Mahmoudpour, M. de la Guardia, J.E.N. Dolatabadi, A. Jouyban, Aptamer-functionalized metal organic frameworks as an emerging nanoprobe in the food safety field: promising development opportunities and translational challenges, TrAC, Trends Anal. Chem. 116622 (2022).
[51] E.M. McConnell, J. Nguyen, Y. Li, Aptamer-based biosensors for environmental monitoring, Front. Chem. 8 (2020) 434.
[52] Z. Wang, et al., NH 2-Ni-MOF electrocatalysts with tunable size/morphology for ultrasensitive C-reactive protein detection via an aptamer binding induced DNA walker–antibody sandwich assay, J. Mater. Chem. B 6 (2018) 2426–2431.
[53] X. Zhang, et al., 2D-porphrinic covalent organic framework-based aptasensor with enhanced photoelectrochemical response for the detection of C-reactive protein, Biosens. Bioelectron. 129 (2019) 64–71.
[54] K.M. Omer, M. Sartin, Dual-mode colorimetric and fluorometric probe for ferric ion detection using N-doped carbon dots prepared via hydrothermal synthesis followed by microwave irradiation, Opt. Mater. 94 (2019).
[55] K.M. Omer, A.Q. Hassan, Chelation-enhanced fluorescence of phosphorus doped carbon nanodots for multi-ion detection, Microchim. Acta 184 (2017).
[56] X. Li, et al., Three hidden talents in one framework: a terephthalic acid-coordinated cupric metal–organic framework with cascade cysteine oxidase-and peroxidase-mimicking activities and stimulus-responsive fluorescence for cysteine sensing, J. Mater. Chem. B 6 (2018) 6207–6211.
[57] X. Tan, et al., Biomineralized Mn3 (PO4) 2/aptamer nanosheets for enhanced electrochemical determination of C-reactive protein, Sensor. Actuator. B Chem. 333 (2021), 129510.
[58] E.D. Bernard, K.C. Nguyen, M.C. DeRosa, A.F. Tayabali, R. Aranda-Rodriguez, Development of a bead-based aptamer/antibody detection system for C-reactive protein, Anal. Biochem. 472 (2015) 67–74.
[59] B. Wu, et al., A simple label-free aptamer-based method for C-reactive protein detection, Anal. Methods 8 (2016) 4177–4180.
[60] W.-C. Kao, C.-H. Chu, W.-H. Chang, Y.-L. Wang, G.-B. Lee, Dual-aptamer assay for C-reactive protein detection by using field-effect transistors on an integrated microfluidic system, in: 2016 IEEE 11th Annual International Conference on Nano/Micro Engineered and Molecular Systems (NEMS) 583–586 (IEEE, 2016.
[61] S. Centi, L. Bonel Sanmartin, S. Tombelli, I. Palchetti, M. Mascini, Detection of C Reactive protein (CRP) in serum by an electrochemical aptamer-based sandwich assay, Electroanalysis: Int. J. Devoted Fund. Pract. Apects Electroanal. 21 (2009) 1309–1315.